

Controlled Topological Structure of Copolyphosphates by Adjusting Pendant Groups of Cyclic Phosphate Monomers

Jinyao Liu,[†] Yan Pang,[†] Wei Huang,* Xiang Zhai, Xinyuan Zhu, Yongfeng Zhou, and Deyue Yan*

School of Chemistry and Chemical Engineering, State Key Laboratory of Metal Matrix Composites, Shanghai Jiao Tong University, 800 Dongchuan Road, Shanghai 200240, P. R. China. [†]These authors are joint first authors.

Received July 14, 2010; Revised Manuscript Received September 13, 2010

ABSTRACT: A convenient method was reported to control the topological structure of copolyphosphates by adjusting the pendant group of cyclic phosphate monomers (CPMs) in the ring-opening polymerization (ROP), including linear block, star block, and hyperbranched multiarm structure. Linear block copolyphosphate (PEP-*b*-PIPP) was prepared by a two-step ROP procedure of CPMs with different pendant groups, i.e., monofunctional propargyl alcohol first initiated the ROP of the CPM with ethyl and then the CPM with isopropyl in turn. Similarly, star block copolyphosphate (SPEP-*b*-PIPP) was also synthesized when the monofunctional propargyl alcohol was replaced by a trifunctional trimethylolpropane. When the pendant group of CPM was changed into 2-hydroxyethyl, hyperbranched polyphosphate (HPHEP) was obtained first through the self-condensing ring-opening polymerization (SCROP) of such CPM, and then the terminal hydroxyls of HPHEP further initiated the ROP of CPM with ethyl to produce hyperbranched multiarm copolyphosphate (HPHEP-*star*-PEP). The resulting copolyphosphates were characterized by NMR, GPC, FTIR, and DSC techniques in detail, and the results confirmed their topological structures. Moreover, methyltetrazolium assay and AO/EB double staining methods indicated that all copolyphosphates with different topological structures had excellent biocompatibility against NIH 3T3 cells and would be applied as novel biomedical materials.

Introduction

Since the topological structures of polymers have significantly influenced their properties, many polymer chemists make great efforts to find novel and facile methods to prepare polymers with different topological structures.^{1–9} Polyphosphates have received great attention in the past few years owing to their good biocompatibility, biodegradability, and the structural similarity to nucleic and teichoic acids.^{10–14} Up to now, many block copolymers containing linear polyphosphate block with various pendant groups have been produced and applied in therapeutic fields.¹⁵ Recently hyperbranched polyphosphates have also been prepared and used for drug delivery.^{16–19} However, copolyphosphates including two or more kinds of phosphate units with various pendant groups in backbone are very intriguing for their specificities and reported seldom.^{20–22} Therefore, it would be highly desirable to prepare copolyphosphates with tunable topological structures from linear to hyperbranched ones.

Generally, various topological structures of polymers can be obtained by adjusting the polymerization conditions or using the specially designed monomers.^{23–27} As to cyclic phosphate monomers (CPMs), they exhibit good flexibility of their pendant groups based on the pentavalent phosphorus.²⁸ Thereby, we want to find an easy way to adjust the topological structure of copolyphosphates. Here we cannot help mentioning the elegant approach presented by Fréchet and Hedrick to prepare hyperbranched polyesters, i.e., self-condensing ring-opening polymerization (SCROP) of cyclic esters,^{29,30} as well as Penczek and co-workers, who pioneered the ring-opening polymerization (ROP) of CPMs

to synthesize linear polyphosphates.^{31–34} It is obvious that the ROP of cyclic monomers is one of the very effective approaches to control the topological structure of polymers. In this paper, we reported a convenient method to control the topological structures of copolyphosphates from linear block to hyperbranched multiarm one, i.e., adjusting the pendant group of CPMs. The schematic synthetic process of copolyphosphates with various topological structures is shown in Scheme 1.

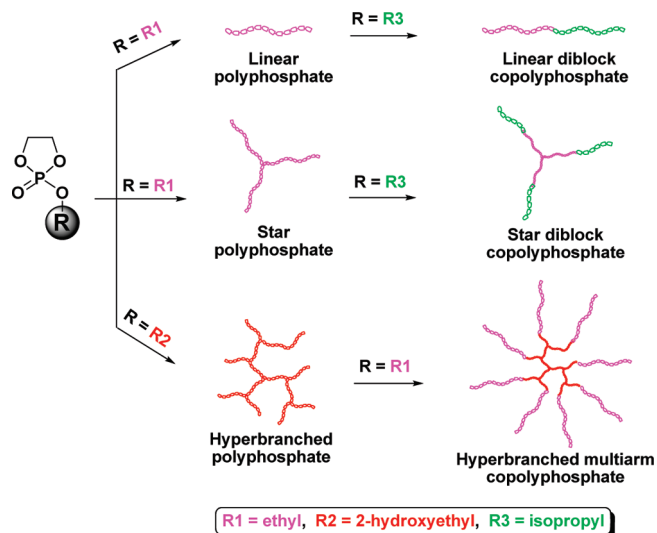
Experimental Section

Materials. 2-Chloro-2-oxo-1,3,2-dioxaphospholane (COP), 2-ethoxy-2-oxo-1,3,2-dioxaphospholane (EP), and 2-isopropoxy-2-oxo-1,3,2-dioxaphospholane (IPP) were synthesized according to the method described previously and distilled under reduced pressure just before use.^{35,36} Propargyl alcohol and *N,N*-dimethylformamide (DMF) were dried over calcium hydride and then purified by vacuum distillation. Triethylamine (TEA) was refluxed with phthalic anhydride, potassium hydroxide, and calcium hydride in turn and distilled just before use. Tetrahydrofuran (THF) and toluene were dried by refluxing with the fresh sodium–benzophenone complex under N₂ and distilled just before use. Ethylene glycol was purified by vacuum distillation. Stannous octoate (Sn(Oct))₂, 1,8-diazabicyclo[5.4.0]undec-7-ene (DBU), trimethylolpropane, and 3-(4,5-dimethylthiazol-2-yl)-2,5-diphenyltetrazolium bromide (MTT) were purchased from Sigma and used as received. Clear polystyrene tissue culture treated 12-well and 96-well plates were obtained from Corning Costar. All other reagents and solvents were purchased from the domestic suppliers and used as received.

Measurements. Nuclear magnetic resonance (NMR) analyses were recorded on a Varian Mercury Plus 400 MHz spectrometer

*Corresponding author. E-mail: hw66@sjtu.edu.cn.

Scheme 1. Schematic Illustration for Controlling the Topological Structure of Copolyphosphates



with deuterated dimethyl sulfoxide (d_6 -DMSO) and deuterated chloroform ($CDCl_3$) as solvents. Gel permeation chromatography (GPC) was performed on a Perkin-Elmer series 200 system (10 μ m PL gel 300 \times 7.5 mm mixed-B and mixed-C column) equipped with a refractive index (RI) detector. DMF containing 0.01 mol/L lithium bromide was used as the mobile phase at a flow rate of 1 mL/min at 70 °C. Fourier transform infrared spectrometer (FTIR) spectra were recorded on a Paragon 1000 instrument by the KBr sample holder method. Differential scanning calorimeter (DSC) was performed on a Perkin-Elmer Pyris 1 in nitrogen atmosphere. An indium standard was used for temperature and enthalpy calibrations. All the samples were first heated from room temperature to 150 °C and held at this temperature for 3 min to eliminate the thermal history, and then they were quenched to -80 °C and heated again from -80 to 150 °C at 10 °C/min.

Synthesis of Poly(2-ethoxy-2-oxo-1,3,2-dioxaphospholane) (PEP). PEP was prepared by the ROP of EP with propargyl alcohol as the initiator and $Sn(Oct)_2$ as the catalyst. The typical polymerization proceeded as follows: propargyl alcohol (61.4 mg, 1.10 mmol), EP (5.00 g, 32.9 mmol), and 20 mL of THF were added to a 25 mL flask in a glovebox with the water content less than 0.1 ppm. Then, $Sn(Oct)_2$ (222 mg, 0.548 mmol) were also added into the flask. The reaction mixture was placed in an oil bath at 35 °C for 3 h. The solution was precipitated into cold diethyl ether containing 10% methanol (v/v) twice. Finally, the purified PEP was obtained by vacuum-drying overnight; yield 78.2%.

Synthesis of Poly(2-ethoxy-2-oxo-1,3,2-dioxaphospholane)-*b*-poly(2-isopropoxy-2-oxo-1,3,2-dioxaphospholane) (PEP-*b*-PIPP). PEP-*b*-PIPP was prepared by the ROP of IPP with PEP as the macroinitiator and DBU as the catalyst. The typical polymerization proceeded as follows: PEP (309 mg, 0.030 mmol) and DBU (22.8 mg, 0.150 mmol) were added into a 10 mL flask in a glovebox with the water content less than 0.1 ppm. The flask was then cooled to 0 °C in an ice bath. Subsequently, IPP (1.67 g, 10 mmol) was added into the flask by a syringe. The reaction mixture was kept stirring at 0 °C for 5 h and then diluted by chloroform. The solution was precipitated into cold diethyl ether containing 10% methanol (v/v) twice. Finally, the purified PEP-*b*-PIPP was obtained by vacuum-drying overnight; yield 63.2%.

Synthesis of 3-Arm Star PEP (SPEP). SPEP was prepared by the ROP of EP with trimethylolpropane as the initiator and $Sn(Oct)_2$ as the catalyst. The typical polymerization proceeded as follows: trimethylolpropane (93.0 mg, 0.694 mmol), EP

(4.225 g, 27.8 mmol), and 10 mL of THF were added to a 25 mL flask in a glovebox with the water content less than 0.1 ppm. Then, $Sn(Oct)_2$ (422 mg, 1.04 mmol) were also added into the flask. The reaction mixture was placed in an oil bath at 35 °C for 4 h. The solution was precipitated into cold diethyl ether containing 10% methanol (v/v) twice. Finally, the purified SPEP was obtained by vacuum-drying overnight; yield 75.6%.

Synthesis of SPEP-*b*-PIPP. SPEP-*b*-PIPP was prepared by the ROP of IPP with SPEP as the macroinitiator and DBU as the catalyst. The typical polymerization proceeded as follows: SPEP (500 mg, 0.116 mmol) and DBU (55.0 mg, 0.362 mmol) were added into a 10 mL flask in a glovebox with the water content less than 0.1 ppm. The flask was then cooled to 0 °C in an ice bath. Subsequently, IPP (2.00 g, 12.0 mmol) was added into the flask by a syringe. The reaction mixture was kept stirring at 0 °C for 1.5 h and then diluted by chloroform. The solution was precipitated into cold diethyl ether containing 10% methanol (v/v) twice. Finally, the purified SPEP-*b*-PIPP was obtained by vacuum-drying overnight; yield 73.8%.

Synthesis of 2-Hydroxyethoxy-2-oxo-1,3,2-dioxaphospholane (HEP). COP (18.0 g, 0.126 mol) in 100 mL of THF was added dropwise over 2 h into a solution of ethylene glycol (7.81 g, 0.126 mol) and TEA (12.8 g, 0.126 mol) in 100 mL of THF under magnetic stirring at -20 °C in a low-temperature thermostatic bath. Then the mixture was kept stirred at -20 °C overnight, and the precipitate was filtered off using a Schlenk funnel with dried silica gel. The filtrate was evaporated under vacuum to obtain some transparent and colorless oil; yield 92.3%.

Synthesis of Hyperbranched Poly(2-hydroxyethoxy-2-oxo-1,3,2-dioxaphospholane) (HPHEP). The SCROP of HEP in bulk was performed in a glovebox with the water content less than 0.1 ppm. HEP (10.0 g, 59.5 mmol) was introduced into a 25 mL flask and stirred by a magnetic bar in an oil bath at 40 °C for 72 h. The resulting product was dissolved in 20 mL of DMSO and dialyzed against DMSO for 72 h and then dialyzed against water for 24 h. After dialysis, the polymer solution was frozen and lyophilized by a freeze-dryer system (Martin Christ, $\alpha 1-4$, Germany) at -20 °C for 48 h. Some transparent viscous hyperbranched polyphosphates HPHEP with terminal hydroxyls was obtained; yield 72.5%.

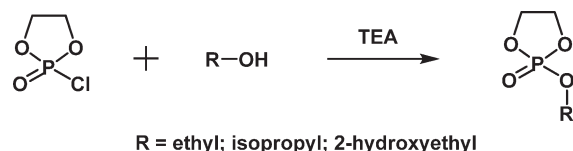
Synthesis of HPHEP-*star*-PEP. HPHEP-*star*-PEP was prepared by the ROP of EP with HPHEP as the macroinitiator and $Sn(Oct)_2$ as the catalyst. The typical polymerization proceeded as follows: HPHEP (0.208 g, 1.24 mmol of hydroxyl), EP (1.89 g, 12.4 mmol), and 4 mL of dry DMF were added to a 10 mL flask in a glovebox with the water content less than 0.1 ppm. Then, $Sn(Oct)_2$ (251 mg, 0.620 mmol) were also added into the flask. The reaction mixture was placed in an oil bath at 35 °C for 3 h. The solution was precipitated into cold diethyl ether containing 10% methanol (v/v). The obtained product was dissolved in chloroform and precipitated in diethyl ether. Finally, the purified HPHEP-*star*-PEP was obtained by vacuum-drying overnight; yield 68.5%.

Cell Culture. NIH 3T3 cells (a mouse embryonic fibroblast cell line) were cultivated in DMEM (Dulbecco's modified Eagle's medium) containing 10% FBS (fetal bovine serum) and antibiotics (50 units/mL penicillin and 50 units/mL streptomycin) at 37 °C in a humidified atmosphere containing 5% CO_2 .

Cytotoxicity Measurements. The relative cytotoxicity of PEP-*b*-PIPP, SPEP and HPHEP-*star*-PEP was estimated by MTT viability assay and AO/EB double staining methods against NIH 3T3 cells.

MTT Assay. NIH 3T3 cells were seeded into 96-well plates at 8×10^3 cells per well in 200 μ L of DMEM. After 24 h incubation, the culture medium was removed and replaced with 200 μ L of DMEM containing serial dilutions of the polymers. The cells were grown for another 24 h. Then, 20 μ L of 5 mg/mL MTT assays stock solution in phosphate buffered saline (PBS) was added to each well. After incubating the cells for 4 h, the medium containing unreacted MTT was removed carefully. The obtained

Scheme 2. Synthetic Routes of CPMs with Different Pendant Groups



blue formazan crystals were dissolved in 200 μL /well DMSO, and the absorbance was measured in a BioTek Elx800 at a wavelength of 490 nm.

AO/EB Double Staining. NIH 3T3 cells were seeded in 6-well plates at 5×10^5 cells per well in 1 mL of complete DMEM and cultured for 24 h, followed by removing culture medium and adding 1 mL of copolyphosphate solution of DMEM with the concentration of 2500 $\mu\text{g}/\text{mL}$. After 24 h incubation, cells were rinsed by PBS twice and incubated in PBS containing AO (5 $\mu\text{g}/\text{mL}$) and EB (5 $\mu\text{g}/\text{mL}$) at 37 $^\circ\text{C}$ in 5% CO_2 for 10 min. Live and dead cells were imaged by an OLYMPUS BX61 fluorescence microscope.

Results and Discussion

Synthesis of CPMs. Because of the high reactivity of chlorine atom in COP, it is often used as the precursor to react with the alcoholic hydroxyl and produce CPMs with different pendant groups. The synthetic route of CPMs with different pendant groups is shown in Scheme 2. EP and IPP are easily obtained through the reaction of COP with ethanol and isopropanol, respectively.^{19,36} In order to obtain the CPM with a hydroxyethyl pendant group, ethylene glycol was used to react with COP. Because of the high reactivity, here COP in THF should be slowly dropped into ethylene glycol in THF at $-20\text{ }^\circ\text{C}$ with TEA as a deacid reagent to ensure only one alcoholic hydroxyl in ethylene glycol molecule reacted with one COP. Moreover, the resulting HEP was not suitable to be purified by the further postprocess because of its relatively low stability. The ^1H , ^{13}C , and ^{31}P NMR spectra of the resulting HEP are exhibited in Figure 1. The peaks at 4.38, 3.98, and 3.54 ppm in Figure 1A are assigned to the protons of $-\text{OCH}_2\text{CH}_2\text{O}-$, $-\text{OCH}_2\text{CH}_2\text{OH}$, and $-\text{OCH}_2\text{CH}_2\text{OH}$, respectively. It is found easily that the ratio of area integration of these peaks is very close to 2:1:1 and well coincides with the molecular structure of HEP. In other words, only one alcoholic hydroxyl in ethylene glycol molecule is confirmed to react with one COP to form HEP monomer at the current reaction condition. In addition, the signals at 70.35, 67.05, and 60.72 ppm (Figure 1B) are attributed to the various carbons of $-\text{OCH}_2\text{CH}_2\text{OH}$, $-\text{OCH}_2\text{CH}_2\text{O}-$, and $-\text{OCH}_2\text{CH}_2\text{OH}$. Furthermore, only one strong resonance at 18.16 ppm appears in the ^{31}P NMR spectrum of HEP (Figure 1C) and verifies there is one kind of phosphorus atom existing in HEP molecules. All the above NMR results sustain that HEP is synthesized successfully.

Synthesis of Linear Block Copolyphosphate. In order to synthesize PEP-*b*-PIPP, a two-step ROP procedure of EP and IPP in turn was conducted with a monofunctional initiator. According to Wang and co-workers' reports, the $\text{Sn}(\text{Oct})_2$ catalytic system can control the ROP of EP well to produce linear polyphosphate at the mild temperature.³⁷ However, the ROP of IPP by using the same catalytic system needs higher temperature and longer time due to the steric hindrance of isopropyl and often goes with some side reactions. So it is difficult to prepare the PIPP block of linear copolyphosphate by using this catalytic system. Fortunately, Iwasaki et al. recently have reported some organocatalysts to proceed the ROP of IPP and produced linear well-defined polyphosphate with narrow molecular weight distribution at

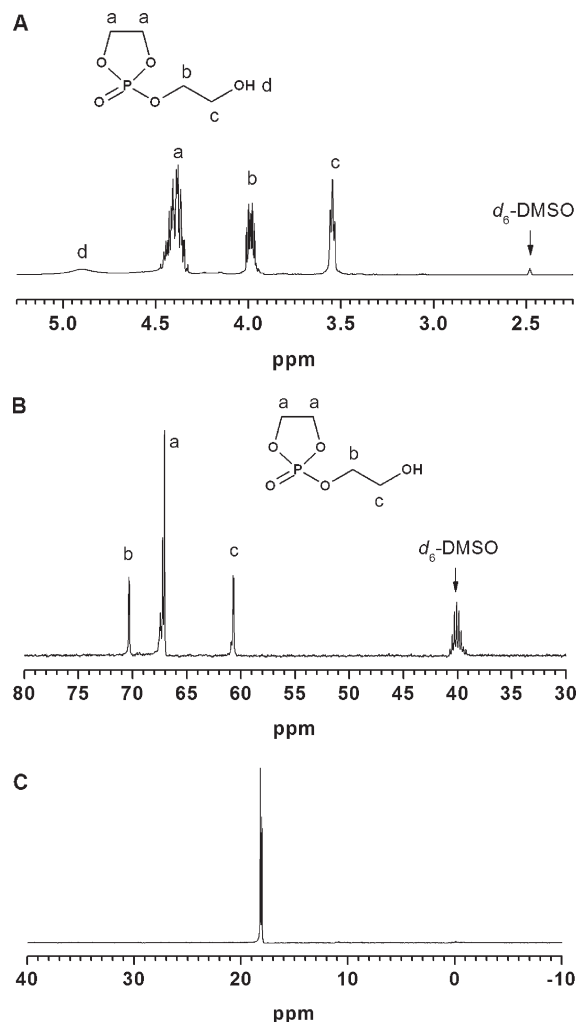


Figure 1. ^1H (A), ^{13}C (B), and ^{31}P (C) NMR spectra of HEP in d_6 -DMSO.

lower temperature.³⁸ Moreover, it is a convenient approach to prepare polymers with unique end functional groups by using functional initiator for the ROP of cyclic monomers. In order to introduce alkynes group to the end of polyphosphates for further application, here propargyl alcohol was selected as the initiator. First, propargyl alcohol and $\text{Sn}(\text{Oct})_2$ were separately used as the initiator and the catalyst to prepare linear polyphosphate PEP by the ROP of EP in THF. Then, the PEP was further used as the macroinitiator and DBU as the organocatalyst to carry out the ROP of IPP in bulk and produced the linear block copolyphosphate PEP-*b*-PIPP. The detailed synthesis route is shown in Scheme 3a.

The chemical structure of PEP-*b*-PIPP was first identified by the ^1H NMR, ^{13}C NMR, and ^{31}P NMR spectra. Comparing the ^1H NMR spectra of PEP and PEP-*b*-PIPP in Figure 2, the new signal is easily observed at 4.65 ppm in the spectrum of PEP-*b*-PIPP, which is assigned to the protons of $-\text{OCH}(\text{CH}_3)_2$ in the PIPP block.^{20,21} The other signals at 4.20, 4.14, and 1.32 ppm are separately attributed to the protons of $-\text{OCH}_2\text{CH}_2\text{O}-$, $-\text{OCH}_2\text{CH}_3$, and $-\text{OCH}_2\text{CH}_3$.³⁶ Furthermore, in contrast to the ^{13}C NMR spectrum of PEP, the new signals which emerged at 73.8 and 23.8 ppm in the spectrum of PEP-*b*-PIPP are attributed to the carbons of $-\text{OCH}(\text{CH}_3)_2$ and $-\text{OCH}(\text{CH}_3)_2$, respectively. The detailed assignments of all signals for various carbon atoms are shown in Supporting Information Figure S1. Moreover, two strong resonances appear at -0.22 and -1.12 ppm in the ^{31}P NMR

spectrum of PEP-*b*-PIPP in Figure 3 are assigned to the phosphorus atoms of PEP and PIPP blocks, respectively.

The molecular weights and polydispersity indexes (PDIs) of PEP and PEP-*b*-PIPP were first measured by GPC. As shown in Figure 4A, the representative GPC profiles of PEP

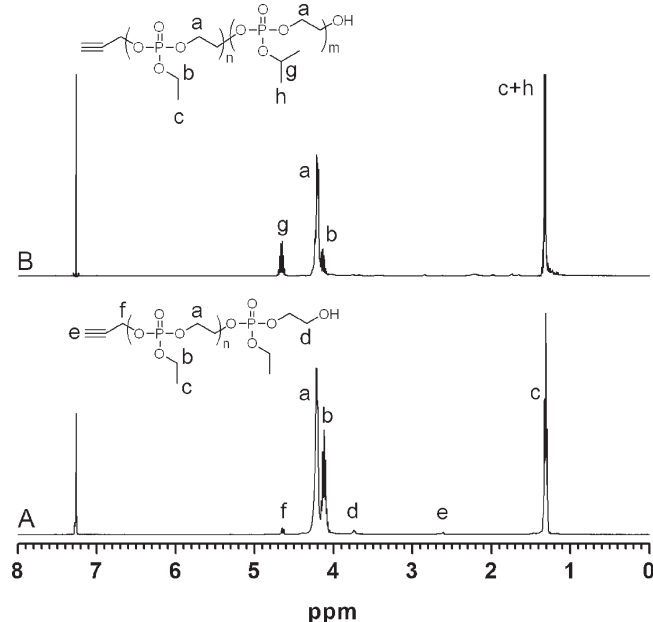


Figure 2. ^1H NMR spectra of PEP (A) and PEP-*b*-PIPP (B) in CDCl_3 .

and PEP-*b*-PIPP are relatively monomodal and symmetric. The curve of PEP-*b*-PIPP shifts clearly toward the direction of high molecular weight, whereas no homopolymer of PIPP can be detected. The number-average molecular weights of PEP and PEP-*b*-PIPP are 10 190 and 24 490 g/mol with relative narrow PDI values of 1.33 and 1.31, respectively. Furthermore, the number-average molecular weights of PEP and PEP-*b*-PIPP are also calculated according to ^1H NMR

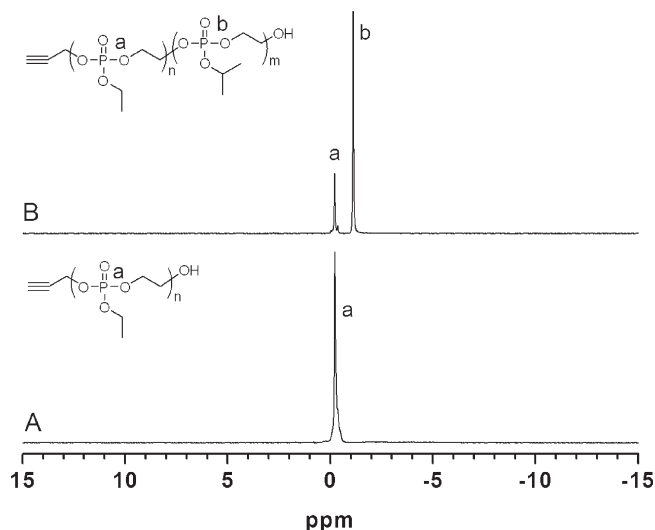
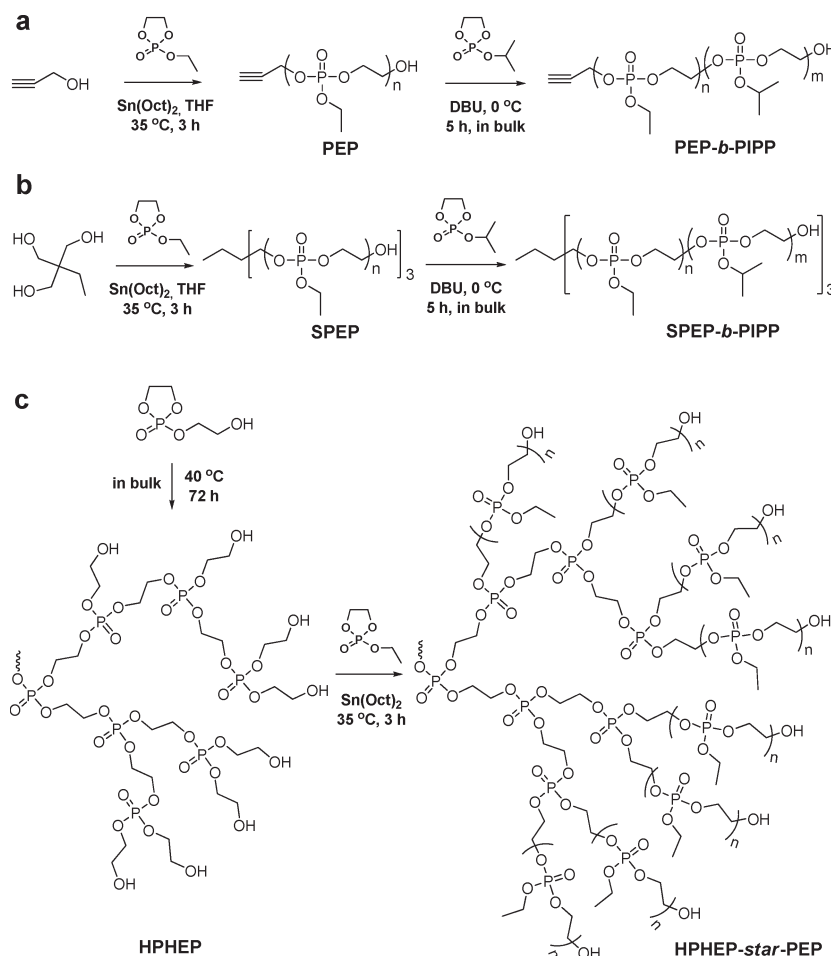


Figure 3. ^{31}P NMR spectra of PEP (A) and PEP-*b*-PIPP (B) in CDCl_3 .

Scheme 3. Detailed Synthetic Routes of PEP-*b*-PIPP (a), SPEP-*b*-PIPP (b), and HPHEP-*star*-PEP (c)



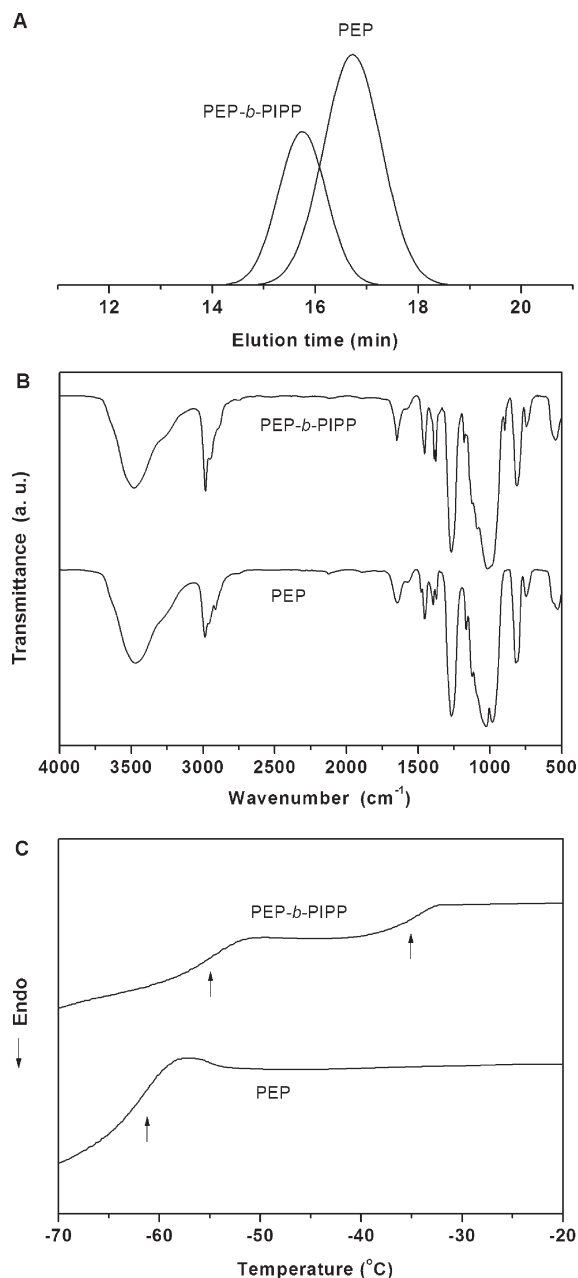


Figure 4. Representative FTIR spectra (A), GPC profiles (B), and DSC curves (C) of PEP and PEP-*b*-PIPP.

spectra, and the results are about 2790 and 6740 g/mol, respectively. Apparently, the results determined by GPC are much higher than those of ¹H NMR analysis, which might be attributed to the strong intermolecular interaction and aggregation of the polyphosphate chains in DMF of the GPC system. The FTIR spectrum and DSC measurement were further used to characterize of PEP-*b*-PIPP. As exhibited in the FTIR spectrum of PEP-*b*-PIPP (Figure 4B), the absorptions at 1268 and 1178 cm⁻¹ can be attributed to the asymmetrical and symmetrical P=O stretching, respectively.¹⁸ The P—O—C stretching is also found at 986 cm⁻¹. In contrast to the FTIR spectrum of PEP, the peaks at 1385 and 1375 cm⁻¹ are the characteristic absorptions of isopropyl stretching to prove the presence of PIPP segments. In addition, two thermal transitions at -54.3 and -34.8 °C were found in the DSC curve of PEP-*b*-PIPP and ascribed to the glass transition of PEP and PIPP blocks, respectively (Figure 4C). All the results of PEP and PEP-*b*-PIPP are

Table 1. Characterization Data of the Resulting Polymers

samples	M_w^a	M_n^a	M_n^b	M_w/M_n^a	yield (%)	T_g^c (°C)
PEP	13580	10190	2790	1.33	78.2	-61.8
PEP- <i>b</i> -PIPP	32240	24490	6740	1.31	63.1	-54.3/-34.8
SPEP	17070	12930	4320	1.32	75.6	-63.5
SPEP- <i>b</i> -PIPP	54320	42110	13930	1.29	73.8	-57.0/-46.3
HPHEP	7650	5760		1.33	72.5	-52.4
HPHEP- <i>star</i> -PEP	22560	8690		2.59	68.6	-53.6

^a Determined by GPC. ^b Calculated on the basis of ¹H NMR results.

^c Measured by DSC.

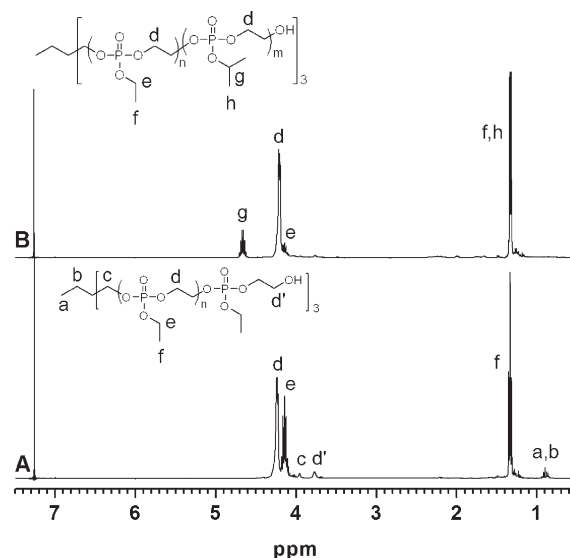


Figure 5. ¹H NMR spectra of SPEP (A) and SPEP-*b*-PIPP (B) in CDCl₃.

summarized in Table 1 and well confirm the block structure of PEP-*b*-PIPP.

Synthesis of Star Block Copolyphosphate. In order to prepare SPEP-*b*-PIPP, a two-step ROP procedure of EP and IPP in turn was performed with a trifunctional initiator. We first used trimethylolpropane as the initiator and Sn(Oct)₂ as the catalyst to prepare 3-arm star polyphosphate SPEP by the ROP of EP in THF. Then, we used SPEP as the macro-initiator and DBU as the organocatalyst to synthesize the star block SPEP-*b*-PIPP by the ROP of IPP in bulk. The detailed synthesis route is given in Scheme 3b.

As shown in Figure 5A, the resonances at 4.23, 4.14, 3.77, and 1.33 ppm in the ¹H NMR spectrum of SPEP are assigned to the protons of —OCH₂CH₂O—, —OCH₂CH₃, —OCH₂CH₂OH, and —OCH₂CH₃, respectively. It is worth noticing that the weak peaks around 3.96 ppm (—C(CH₂OP—)₃) and 0.90 ppm (CH₃CH₂C— and CH₃CH₂C—) are appointed to the protons of the initiator trimethylolpropane. This result confirms the successful initiation of EP by trimethylolpropane to generate SPEP with the 3-arm star structure. The ¹H NMR spectrum of SPEP-*b*-PIPP is displayed in Figure 5B, and the new signal at 4.65 ppm is simply assigned to the protons of —OCH(CH₃)₂ in the PIPP block. The star structures of SPEP and SPEP-*b*-PIPP were further confirmed by ¹³C NMR and ³¹P NMR spectra. Their ¹³C NMR spectra are shown in Supporting Information Figure S2, and all signals for various carbon atoms are assigned in detail. It is obvious that a weak and a strong resonances appeared at 0.58 and -0.23 ppm in the ³¹P NMR spectrum of SPEP, which assigned to the phosphorus atoms in the backbone and the

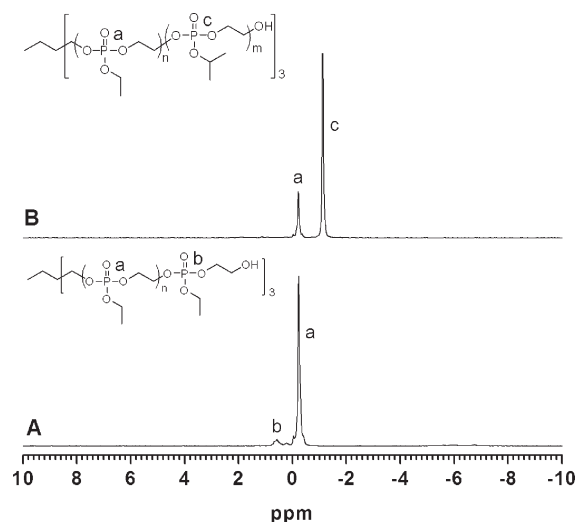


Figure 6. ^{31}P NMR spectra of SPEP (A) and SPEP-*b*-PIPP (B) in CDCl_3 .

end of PEP chains, respectively (Figure 6A).³⁷ In the ^{31}P NMR spectrum of SPEP-*b*-PIPP (Figure 6B), there are two strong peaks at -0.23 and -1.13 ppm naturally attributed to the phosphorus atoms in PEP and PIPP blocks, respectively. However, the resonance of phosphorus atom at the end of PIPP blocks is not detected. This can be ascribed to the molar ratio of terminal phosphorus in SPEP-*b*-PIPP becoming very low with the molecular weight increased after grafting PIPP blocks to SPEP. Moreover, the molecular weights and PDI values of SPEP and SPEP-*b*-PIPP were also analyzed by GPC and ^1H NMR. As shown in Table 1, the number-average molecular weights of SPEP and SPEP-*b*-PIPP are 12 930 and 42 110 g/mol with PDI values of 1.32 and 1.29 by GPC, respectively. Furthermore, they are about 4320 and 13 930 g/mol, respectively, calculated on the basis of ^1H NMR spectra. Because of the same reasons of PEP and PEP-*b*-PIPP, the results determined by GPC are also much higher than those by ^1H NMR analysis. Similarly, all the characteristic absorptions attributed to $\text{P}=\text{O}$, $\text{P}-\text{O}-\text{C}$, and isopropyl stretching are detected in the FTIR spectrum of SPEP-*b*-PIPP (Supporting Information Figure S3). Two glass transitions at -57.0 and -46.3 °C are observed in the DSC curve of SPEP-*b*-PIPP and attributed to SPEP and PIPP blocks, respectively (Table 1). All above results confirm the star block structure of SPEP-*b*-PIPP.

Synthesis of Hyperbranched Multiarm Copolyphosphate. According to our previous reported approach, polyphosphate with a hyperbranched structure can be facile synthesized through SCROP of a hydroxyl-functionalized CPM.¹⁶ Hyperbranched polyphosphate of HPHEP with many terminal hydroxyl groups was easily prepared by SCROP of HEP in bulk without catalyst at 40 °C for 72 h. Then, hyperbranched multiarm copolyphosphate of HPHEP-*star*-PEP was produced through ROP of EP by using HPHEP as the macroinitiator and $\text{Sn}(\text{Oct})_2$ as the catalyst (Scheme 3c).

The ^1H NMR spectra of HPHEP and HPHEP-*star*-PEP are shown in Figure 7. The peaks at 4.19, 3.98, and 3.56 ppm in the spectrum of HPHEP are separately assigned to protons of $-\text{OCH}_2\text{CH}_2\text{O}-$, $-\text{OCH}_2\text{CH}_2\text{OH}$, and $-\text{OCH}_2\text{CH}_2\text{OH}$ (Figure 7A). The weak and broad peak at 4.90 ppm is attributed to the terminal hydroxyl groups in HPHEP. Comparing to that of HPHEP, the newly observed peaks at 4.05 and 1.24 ppm in the spectrum of HPHEP-*star*-PEP are easily assigned to the protons of $-\text{OCH}_2\text{CH}_3$ and $-\text{OCH}_2\text{CH}_3$ in the PEP arms, respectively (Figure 7B). The peaks at 3.95 and 3.55 ppm are assigned to the methylene protons

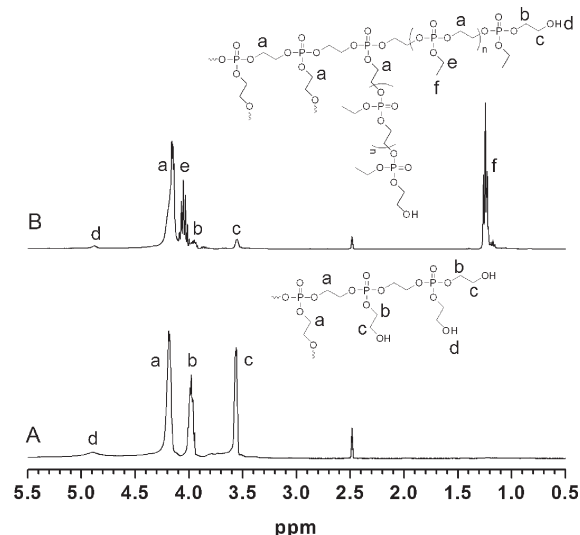


Figure 7. ^1H NMR spectra of HPHEP (A) and HPHEP-*star*-PEP (B) in d_6 -DMSO.

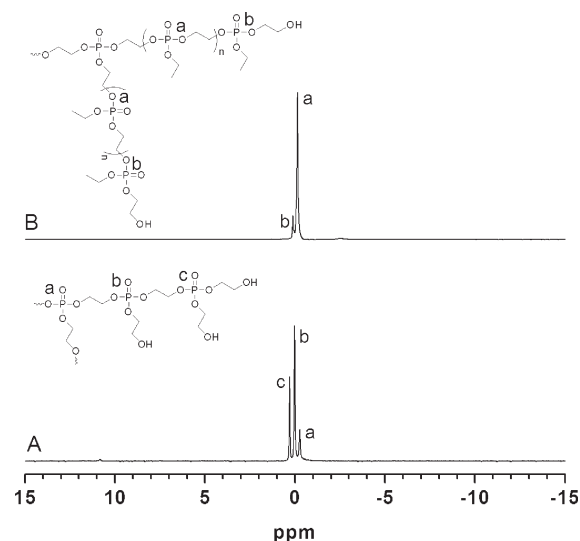


Figure 8. ^{31}P NMR spectra of HPHEP (A) and HPHEP-*star*-PEP (B) in d_6 -DMSO.

of $-\text{OCH}_2\text{CH}_2\text{OH}$ and $-\text{OCH}_2\text{CH}_2\text{OH}$ at the end of PEP arms. The average degree of polymerization of the PEP arms is about 6 by calculating the relative intensity of the peak at 3.55 ppm (the methylene groups adjacent to the terminal hydroxyl groups in PEP arms) and the peak at 1.24 ppm (the methyl groups in PEP arms). The ^{13}C NMR measurements were further used to verify the structure of HPHEP-*star*-PEP. As assigned in the spectrum of HPHEP-*star*-PEP (Supporting Information Figure S4), the chemical shifts at 69.56, 66.75, 64.41, 60.67, and 18.52 ppm are separately assigned to carbons of $-\text{OCH}_2\text{CH}_2\text{OH}$, $-\text{OCH}_2\text{CH}_2\text{O}-$, $-\text{OCH}_2\text{CH}_3$, $-\text{OCH}_2\text{CH}_2\text{OH}$, and $-\text{OCH}_2\text{CH}_3$. Additionally, three peaks at 0.29, 0.02, and -0.27 ppm in the ^{31}P NMR spectrum of HPHEP (Figure 8A) are attributed to phosphorus atoms in the terminal, linear, and dendritic units, respectively.¹⁶ The degree of branching (DB) of the resulting HPHEP can be calculated according to the corresponding integrals of the peak areas of various structural units in the quantitative ^{31}P NMR spectrum on the basis of the following formula:³⁹

$$\text{DB} = \frac{S_D + S_T}{S_D + S_T + S_L}$$

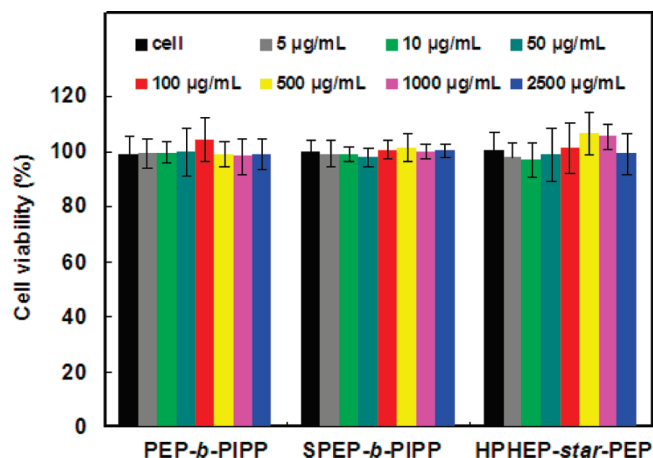


Figure 9. Cell viability of NIH 3T3 cells against PEP-*b*-PIPP, SPEP-*b*-PIPP, and HPHEP-*star*-PEP after cultured for 24 h with the different polymer concentrations determined by MTT assay.

Here S_D is the integral area of dendritic units, S_T the integral area of terminal units, and S_L the integral area of linear units. As a result, the DB of HPHEP is calculated to be 0.46. As displayed in Figure 8B, only a strong peak at -0.15 ppm and a weak peak at 0.11 ppm are observed in the spectrum of HPHEP-*star*-PEP, which are assigned to the phosphorus atoms in PEP arm backbone and arm end, respectively. This is ascribed to the hyperbranched structure of HPHEP core, which makes the molar ratio of phosphorus atoms in the PEP arm ends become large and can be detected clearly. The molecular weights and T_g values of HPHEP and HPHEP-*star*-PEP were further measured by GPC and DSC techniques, respectively, and the results are also summarized in Table 1. Additionally, the FTIR spectrum of HPHEP-*star*-PEP is given in Supporting Information Figure S5. All of these results demonstrate the hyperbranched multiarm structure of HPHEP-*star*-PEP.

In Vitro Cytotoxicity of Copolyphosphates. As a class of eminent biomaterials, linear polyphosphates have been extensively investigated by Leong' and Wang's groups, and their low toxicity to various cultural cell lines has been proved.^{40–43} According to our previous report, hyperbranched polyphosphates as well as their degradation products also have excellent biocompatibility.¹⁸ The *in vitro* cytotoxicity of copolyphosphates of PEP-*b*-PIPP, SPEP-*b*-PIPP, and HPHEP-*star*-PEP against NIH 3T3 cells was first studied using MTT assay. The MTT assay is based on the ability of a mitochondrial dehydrogenation enzyme in viable cells to cleave the tetrazolium rings of the pale yellow MTT and form formazan crystals with dark blue color. Therefore, the number of surviving cells is directly proportional to the level of formed formazan.⁴⁴ As shown in Figure 9, the cell viability after 24 h incubation with copolyphosphates up to $2500 \mu\text{g/mL}$ remains nearly 100% compared with the untreated cells. Evidently, these materials have good biocompatibility to NIH 3T3 cells. Furthermore, the AO/EB double staining results also demonstrate their good biocompatibility. Generally speaking, healthy cells have green nuclei and uniform chromatin with intact cell membrane. On the contrary, the cells undergoing apoptosis have orange nuclei and condensed chromatin with nuclear shrinkage. What is more, the cells in necrosis or in the late stage of apoptosis have red nuclei with damaged cell membrane.⁴⁵ The fluorescence of NIH 3T3 cells after incubated with HPHEP-*star*-PEP of $2500 \mu\text{g/mL}$ for 24 h is almost the same as that of the untreated cells (data not shown), which approves the viability of the cells (Supporting Information, Figure S6).

Conclusions

The topological structures of copolyphosphates were simply controlled through ROP of CPMs by adjusting their pendant groups, including linear block, star block, and hyperbranched multiarm structures. The linear block PEP-*b*-PIPP was prepared by a two-step ROP procedure of EP and IPP in turn with a monofunctional initiator of propargyl alcohol. The ROP of EP was conducted in THF at 35°C for 3 h with $\text{Sn}(\text{Oct})_2$ as catalyst. Then the ROP of IPP was carried out in bulk at 0°C for 5 h using PEP as macroinitiator and DBU as catalyst. The star block SPEP-*b*-PIPP was synthesized similarly to linear block copolyphosphate, except that the initiator was replaced by trifunctional trimethylolpropane. Hyperbranched multiarm HPHEP-*star*-PEP was synthesized by SCROP of HEP and then ROP of EP. The SCROP of HEP was performed in bulk at 40°C for 72 h without catalyst, and the ROP of EP was conducted at 35°C for 3 h using HPHEP as macroinitiator and $\text{Sn}(\text{Oct})_2$ as catalyst. The topological structures of the resulting copolyphosphates were confirmed well by the NMR, GPC, FTIR, and DSC analyses. The molecular weights of PEP-*b*-PIPP, SPEP-*b*-PIPP, and HPHEP-*star*-PEP were 6740, 13 930, and 8690, with PDI values of 1.31, 1.29, and 2.59, respectively. Moreover, MTT assay and AO/EB double staining methods demonstrated that these copolyphosphates have excellent biocompatibility against NIH 3T3 cells. The cell viability after 24 h incubation with copolyphosphates up to $2500 \mu\text{g/mL}$ remained nearly 100% compared with the untreated cells. In summary, the topological structures of these copolyphosphates can be controlled facilely by adjusting the pendant groups of CPMs. All of these copolyphosphates can be used as novel materials in biomedical areas.

Acknowledgment. The authors gratefully acknowledge the financial supports provided by the National Basic Research Program (2007CB808000, 2009CB930400), National Natural Science Foundation of China (No. 50873058, No. 50633010), and Shanghai Leading Academic Discipline Project (No. B202).

Supporting Information Available: ^{13}C NMR and FTIR spectra of copolyphosphates and fluorescence image of NIH 3T3 cells. This material is available free of charge via the Internet at <http://pubs.acs.org>.

References and Notes

- Hawker, C. J.; Fréchet, J. M. J. *ACS Symp. Ser.* **1996**, 624, 132.
- Guan, Z.; Cotts, P. M.; McCord, E. F.; McLain, S. J. *Science* **1999**, 283, 2059.
- Hecht, S.; Fréchet, J. M. J. *Angew. Chem., Int. Ed.* **2001**, 40, 74.
- Kim, Y. H.; Webster, O. W. *J. Am. Chem. Soc.* **1990**, 112, 4592.
- Grayson, S. M.; Fréchet, J. M. J. *Chem. Rev.* **2001**, 101, 3819.
- Jia, Z.; Chen, H.; Zhu, X.; Yan, D. *J. Am. Chem. Soc.* **2006**, 128, 8144.
- Chen, L.; Zhu, X.; Yan, D.; Chen, Y.; Chen, Q.; Yao, Y. *Angew. Chem., Int. Ed.* **2005**, 45, 87.
- Feng, X.; Taton, D.; Borsali, R.; Chaikof, E. L.; Gnanou, Y. *J. Am. Chem. Soc.* **2006**, 128, 11551.
- Saudan, C.; Balzani, V.; Gorka, M.; Lee, S.-K.; Maestri, M.; Vicinelli, V.; Vogtle, F. *J. Am. Chem. Soc.* **2003**, 125, 4424.
- Xu, X.; Yu, H.; Gao, S.; Mao, H.; Leong, K. W.; Wang, S. *Biomaterials* **2002**, 23, 3765.
- Wen, J.; Zhuo, R. *Macromol. Rapid Commun.* **1998**, 19, 641.
- Iwasaki, Y.; Akiyoshi, K. *Biomacromolecules* **2006**, 7, 1433.
- Liu, X.; Ni, P.; He, J.; Zhang, M. *Macromolecules* **2010**, 43, 4771.
- Chen, D.; Wang, J. *Macromolecules* **2006**, 39, 473.
- Wang, Y.; Yuan, Y.; Du, J.; Yang, X.; Wang, J. *Macromol. Biosci.* **2009**, 9, 1154.
- Liu, J.; Huang, W.; Zhou, Y.; Yan, D. *Macromolecules* **2009**, 42, 4394.
- Liu, J.; Pang, Y.; Huang, W.; Zhu, X.; Zhou, Y.; Yan, D. *Biomaterials* **2010**, 31, 1334.

- (18) Liu, J.; Huang, W.; Pang, Y.; Zhu, X.; Zhou, Y.; Yan, D. *Biomacromolecules* **2010**, *11*, 1564.
- (19) Liu, J.; Pang, Y.; Huang, W.; Zhu, X.; Zhou, Y.; Yan, D. *Biomaterials* **2010**, *31*, 5643.
- (20) Iwasaki, Y.; Wachiralarpphaithoon, C.; Akiyoshi, K. *Macromolecules* **2007**, *40*, 8136.
- (21) Wang, Y.; Li, Y.; Yang, X.; Yuan, Y.; Yan, L.; Wang, J. *Macromolecules* **2009**, *42*, 3026.
- (22) Wang, Y.; Tang, L.; Li, Y.; Wang, J. *Biomacromolecules* **2009**, *10*, 66.
- (23) Kageyama, K.; Tamazawa, J.; Aida, T. *Science* **1999**, *285*, 2113.
- (24) Matyjaszewski, K.; Davis, T. P. *Handbook of Radical Polymerization*; John Wiley & Sons: New York, 2002.
- (25) Chen, G.; Ma, X.; Guan, Z. *J. Am. Chem. Soc.* **2003**, *125*, 6697.
- (26) Guan, Z. *J. Am. Chem. Soc.* **2002**, *124*, 5616.
- (27) Hong, C.; You, Y.; Wu, D.; Liu, Y.; Pan, C. *J. Am. Chem. Soc.* **2007**, *129*, 5354.
- (28) Wang, J.; Mao, H.; Leong, K. W. *J. Am. Chem. Soc.* **2001**, *123*, 9480.
- (29) Trollsas, M.; Löwenhielm, P.; Lee, V. Y.; Möller, M.; Müller, R. D.; Hedrick, J. L. *Macromolecules* **1999**, *32*, 9062–9066.
- (30) Liu, M.; Vladimirov, N.; Fréchet, J. M. J. *Macromolecules* **1999**, *32*, 6881–6884.
- (31) Libiszowski, J.; Kaluzynski, K.; Penczek, S. *J. Polym. Sci., Part A: Polym. Chem.* **1978**, *16*, 1275.
- (32) Lapienis, G.; Penczek, S. *J. Polym. Sci., Part A: Polym. Chem.* **1977**, *15*, 371.
- (33) Lapienis, G.; Penczek, S. *Macromolecules* **1977**, *10*, 1301.
- (34) Pretula, J.; Kaluzynski, K.; Penczek, S. *Macromolecules* **1986**, *19*, 1797.
- (35) Edmundson, R. S. *Chem. Ind.* **1962**, 1828.
- (36) Liu, J.; Huang, W.; Pang, Y.; Zhu, X.; Zhou, Y.; Yan, D. *Langmuir* **2010**, *26*, 10585.
- (37) Xiao, C.; Wang, Y.; Du, J.; Chen, X.; Wang, J. *Macromolecules* **2006**, *39*, 6825.
- (38) Iwasaki, Y.; Yamaguchi, E. *Macromolecules* **2010**, *43*, 2664.
- (39) Hawker, C. J.; Lee, R.; Fréchet, J. M. J. *J. Am. Chem. Soc.* **1991**, *113*, 4583.
- (40) Wen, J.; Kim, G. J. A.; Leong, K. W. *J. Controlled Release* **2003**, *92*, 39.
- (41) Wang, S.; Wan, A. C.; Xu, X.; Gao, S.; Mao, H. Q.; Leong, K. W.; Yu, H. *Biomaterials* **2001**, *22*, 1157.
- (42) Wen, J.; Mao, H.; Li, W.; Lin, K. Y.; Leong, K. W. *J. Pharm. Sci.* **2004**, *93*, 2142.
- (43) Wang, Y.; Tang, L.; Sun, T.; Li, C.; Xiong, M.; Wang, J. *Biomacromolecules* **2008**, *9*, 388.
- (44) Mosmann, T. *J. Immunol. Methods* **1983**, *65*, 55.
- (45) Cohen, J. J. *Immunol. Today* **1993**, *14*, 126.